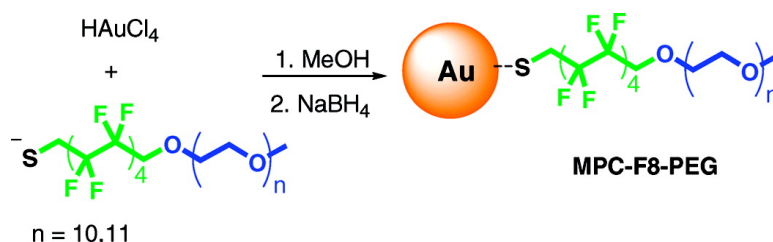


Water-Soluble Gold Nanoparticles Protected by Fluorinated Amphiphilic Thiolates

Cristina Gentilini, Fabrizio Evangelista, Petra Rudolf, Paola Franchi, Marco Lucarini, and Lucia Pasquato

J. Am. Chem. Soc., **2008**, 130 (46), 15678-15682 • DOI: 10.1021/ja8058364 • Publication Date (Web): 25 October 2008

Downloaded from <http://pubs.acs.org> on February 8, 2009



More About This Article

Additional resources and features associated with this article are available within the HTML version:

- Supporting Information
- Access to high resolution figures
- Links to articles and content related to this article
- Copyright permission to reproduce figures and/or text from this article

[View the Full Text HTML](#)

Water-Soluble Gold Nanoparticles Protected by Fluorinated Amphiphilic Thiolates

Cristina Gentilini,[†] Fabrizio Evangelista,[‡] Petra Rudolf,[‡] Paola Franchi,[§]
Marco Lucarini,[§] and Lucia Pasquato^{*†}

Department of Chemical Sciences and INSTM, Trieste Unit, University of Trieste, via L. Giorgieri 1, I-34127 Trieste, Italy, Zernike Institute for Advanced Materials, University of Groningen, Nijenborgh 4, NL-9747 AG Groningen, The Netherlands, and Department of Organic Chemistry "A. Mangini", University of Bologna, via San Giacomo 11, I-40126 Bologna, Italy

Received August 5, 2008; E-mail: lpasquato@units.it

Abstract: The preparation and the properties of gold nanoparticles (Au NPs) protected by perfluorinated amphiphiles are described. The thiols were devised to form a perfluorinated region close to the gold surface and to have a hydrophilic portion in contact with the bulk solvent to impart solubility in water. The monolayer protected clusters were prepared, in an homogeneous phase using sodium thiolates because of the low nucleophilicity of the alpha-perfluorinated thiols, and fully characterized with ¹H, ¹⁹F NMR spectrometry, IR and UV–vis absorption spectroscopies, transmission electron microscopy (TEM), thermogravimetric analysis (TGA), and X-ray photoelectron spectroscopy (XPS). Au NPs with core diameters ranging from 1.6 to 2.9 nm, depending on the reaction conditions, were obtained. Water-soluble NPs (MPC-F8-PEGs) were obtained with the thiol HS-F8-PEG ending with a short poly(ethylene glycol) unit (PEG-OMe 550), whereas thiols with shorter PEG chains give rise to NPs insoluble in water. MPC-F8-PEGs undergo an exchange reaction with amphiphilic alkyl thiols. ESR investigations, using a hydrophobic radical probe, indicate that the MPC-F8-PEG monolayer shows a greater hydrophobicity compared to the analogous hydrogenated monolayer.

Introduction

Gold nanoparticles have captured researchers' attention because of their peculiar properties, their high stability compared to other metal nanoparticles, and also because of their biological compatibility. As a natural consequence "spherical" gold surfaces have been widely used as platforms of choice for 3D self-assembled monolayers (SAMs) in analogy to 2D-SAMs on gold surfaces. The pioneering work by Brust and Schiffrin in 1994 describing the formation of self-assembled monolayers by thiolates around gold clusters¹ has opened the way to 3D SAMs. Indeed, thiolates on gold nanoparticles are the most studied examples of 3D SAMs.² 3D monolayers of alkanethiolates are robust and passivate efficiently the gold surface. The topological organization of thiolates in a 3D SAM may be different from what is known for a 2D SAM as reported for homoligand^{3–6} and heteroligand monolayers.⁷

Several examples of 3D SAMs formed by hydrophilic or amphiphilic thiols to impart solubility in water have been reported.^{8–10} In particular, thiols with this property may be divided into three groups: (i) thiols terminated with an oligo or poly(ethylene glycol) moiety that are employed to form "inert surfaces", resistant to nonspecific adsorption of biomolecules and cells;^{8–10} (ii) simple alkyl thiols with a polar end group such as a carboxylate or an ammonium ion;^{11,12} (iii) biomolecules such as peptides, glycosides, DNA sequences, containing a thiol group or linked to a short alkyl thiol. Differently from

[†] University of Trieste.

[‡] University of Groningen.

[§] University of Bologna.

- (1) Brust, M.; Walker, M.; Bethell, D.; Schiffrin, D. J.; Whyman, R. *J. Chem. Soc., Chem. Commun.* **1994**, 801–802.
- (2) Love, J. C.; Estroff, L. A.; Kriebel, J. K.; Nuzzo, R. G.; Whitesides, G. M. *Chem. Rev.* **2005**, *105*, 1103–1169.
- (3) (a) Luedtke, W. D.; Landman, U. *J. Phys. Chem.* **1996**, *32*, 13323–13329. (b) Luedtke, W. D.; Landman, U. *J. Phys. Chem. B* **1998**, *102*, 6566–6572.
- (4) Ghorai, P. Kr.; Glotzer, S. C. *J. Phys. Chem. C* **2007**, *111*, 15857–15862.
- (5) Gutierrez-Wing, C.; Ascencio, J. A.; Perez-Alvarez, M.; Marin-Almazo, M.; Jose-Yacamán, M. *J. Cluster Sci.* **1998**, *9*, 529–545.

(6) Rapino, S.; Zerbetto, F. *Small* **2007**, *3*, 386–388.

(7) (a) Jackson, A. M.; Myerson, J. W.; Stellacci, F. *Nat. Mater.* **2004**, *3*, 330–336. (b) Jackson, A. M.; Hu, Y.; Silva, P. J.; Stellacci, F. *J. Am. Chem. Soc.* **2006**, *128*, 11135–11149. (c) Singh, C.; Ghorai, P. K.; Horsch, M. A.; Jackson, A. M.; Larson, R. G.; Stellacci, F.; Glotzer, S. C. *Phys. Rev. Lett.* **2007**, *99*, 226106. (d) Carney, R. P.; DeVries, G. A.; Dubois, C.; Kim, H.; Kim, J. Y.; Singh, C.; Ghorai, P. K.; Tracy, J. B.; Stiles, R. L.; Murray, R. W.; Glotzer, S. C.; Stellacci, F. *J. Am. Chem. Soc.* **2008**, *130*, 798–799. (e) Uzun, O.; Hu, Y.; Verma, A.; Chen, S.; Centrone, A.; Stellacci, F. *Chem. Commun.* **2008**, 196–198.

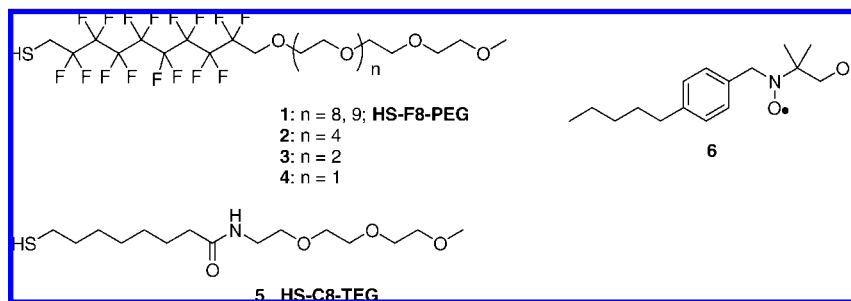
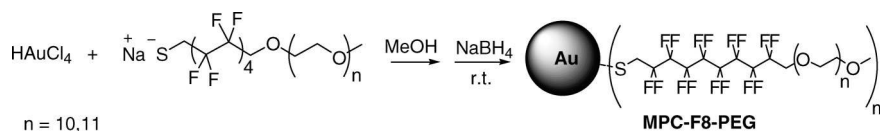
(8) Kanaras, A. G.; Kamounah, F. S.; Schaumburg, K.; Kiely, C. J.; Brust, M. *Chem. Commun.* **2002**, 2294–2295.

(9) Foos, E. E.; Snow, A. W.; Twigg, M. E.; Ancona, M. G. *Chem. Mater.* **2002**, *14*, 2401–2408.

(10) Pengo, P.; Polizzi, S.; Battagliarin, M.; Pasquato, L.; Scrimin, P. *J. Mater. Chem.* **2003**, *13*, 2471–2478.

(11) Jadzinsky, P. D.; Calero, G.; Ackerson, C. J.; Bushnell, D. A.; Kornberg, R. D. *Science* **2007**, *318*, 430–433.

(12) (a) Simard, J.; Briggs, C.; Boal, A. K.; Rotello, V. M. *Chem. Commun.* **2000**, 1943–1944. (b) Sandhu, K. K.; McIntosh, C. M.; Simard, J. M.; Smith, S. W.; Rotello, V. M. *Bioconjugate Chem.* **2002**, *13*, 3–6.

Chart 1. Fluorinated Amphiphilic Thiols 1–4, Amphiphilic Thiol 5, and Nitroxide Radical 6**Scheme 1.** Synthesis of MPC-F8-PEG

the first group of monolayers, the last two categories may display a range of functional groups at the interface and are apt to study cooperativity and polyvalency extending the use of monolayer protected clusters (MPCs) for biosensors^{13–16} and for medical diagnosis and therapies.^{17–20}

Gold nanoparticles passivated by perfluorinated alkylthiols and perfluorinated arylthiols, such as for example commercially available 1*H*,1*H*,2*H*,2*H*-perfluorooctane- and 1*H*,1*H*,2*H*,2*H*-perfluorodecanethiols, have been reported.^{21,22} Because of the presence of the short alkyl chain between the thiol group and the perfluorinated chain, classical procedures for the synthesis of the nanoparticles could be used eventually with trifluorotoluene (instead of toluene) to increase the solubility of the perfluorinated ligands. However, the obtained nanoparticles precipitate from the reaction mixture and could be solubilized in fluorinated solvents only. This hampers purification but allows expansion of the chemistry of metal NPs into the so-called fluoruous phase.

Perfluorinated amphiphiles characterized by a hydrophilic portion that contrasts with the high hydrophobicity of the perfluorocarbon region are soluble in polar solvents. The combination of the known biocompatibility of fluorinated compounds with the solubility properties makes these surfactants

interesting for applications in material science²³ and in the biomedical field.²⁴

The merging of the features of biocompatible water-soluble gold nanoparticles and the properties of polymers or aggregates of perfluorinated amphiphiles will open the way to new biomedical applications, for example, in the field of antioxidant carriers or in the development of multicompartament nanoparticles with the capacity to store and release active molecules. These considerations pushed us to design the first example of water-soluble gold nanoparticles protected by a monolayer of fluorinated amphiphilic thiols (MPC-F8-PEG). For their synthesis, the thiol 1 (HS-F8-PEG) with a perfluorinated portion and a short poly(ethylene glycol) unit (PEG-OMe 550) has been designed and its synthesis described recently by some of us (Chart 1).²⁵ Since the thiol group is in α -position to the perfluorinated chain, it was necessary to modify the known procedures for the synthesis of Au NPs. These nanoparticles are soluble in polar organic solvents and in water and were characterized by TEM, TGA analysis, IR spectra, UV–visible spectra, XPS measurements, and ¹H and ¹⁹F NMR spectra. Moreover, ESR measurements were carried out to study how a hydrophobic radical probe interacts with the fluorinated part of the monolayer and how it compares with MPC-C8-TEG.²⁶ The composition of the monolayer can be modified by an exchange process with amphiphilic alkyl thiols. In addition, nanoparticles protected by fluorinated amphiphilic thiols with tri-, tetra-, or

- (13) Anker, J. N.; Hall, W. P.; Lyandres, O.; Shah, N. C.; Zhao, J.; Van Duyne, R. P. *Nat. Mater.* **2008**, *7*, 442–453.
- (14) (a) Niemeyer, C. M.; Mirkin, C. A., Eds.; *Nanobiotechnology*; Wiley-VCH: Weinheim, 2004. (b) Mirkin, C. A.; Niemeyer, C. M., Eds.; *Nanobiotechnology II*; Wiley-VCH: Weinheim, 2007. (c) Rosi, N. L.; Mirkin, C. A. *Chem. Rev.* **2005**, *105*, 1547–1562.
- (15) (a) You, C.-C.; Chompoosor, A.; Rotello, V. M. *Nanotoday* **2007**, *2*, 34–43. (b) You, C.-C.; Verma, A.; Rotello, V. M. *Soft Matter* **2006**, *2*, 190–204. (c) You, C.-C.; Miranda, O. R.; Gider, B.; Ghosh, P. S.; Kim, I.-B.; Erdogan, B.; Krovi, S. A.; Bunz, U. H. F.; Rotello, V. M. *Nat. Nanotechnol.* **2007**, *2*, 318–323.
- (16) Phillips, R. L.; Miranda, O. R.; You, C.-C.; Rotello, V. M.; Bunz, U. H. F. *Angew. Chem., Int. Ed.* **2008**, *47*, 2590–2594.
- (17) Ghadiali, J. E.; Stevens, M. M. *Adv. Mater.* **2008**, *20*, DOI:10.1002/adma.200703158.
- (18) Skrabalak, S. E.; Chen, J.; Au, L.; Lu, X.; Li, X.; Xia, Y. *Adv. Mater.* **2007**, *19*, 3177–3184.
- (19) De la Fuente, J. M.; Pendés, S. *Biochim. Biophys. Acta* **2006**, *1760*, 636–651.
- (20) Huang, X.; Jain, P. K.; El-Sayed, I. H.; El-Sayed, M. A. *Nanomedicine* **2007**, *2*, 681–693.
- (21) Yonezawa, T.; Onoue, S.; Kimizuka, N. *Langmuir* **2001**, *17*, 2291–2293.
- (22) Dass, A.; Guo, R.; Tracy, J. B.; Balasubramanian, R.; Douglas, A. D.; Murray, R. W. *Langmuir* **2008**, *24*, 310–315.

- (23) (a) Dinglasan-Panlilio, M. J. A.; Mabury, S. A. *Environ. Sci. Technol.* **2006**, *40*, 1447–1453. (b) Thomann, Y.; Haag, R.; Brenn, R.; Delto, R.; Weickman, H.; Thomann, R.; Mülhaupt, R. *Macromol. Chem. Phys.* **2005**, *206*, 135–141. (c) Bleta, R.; Blin, J. L.; Stébé, M. J. *J. Phys. Chem. B* **2006**, *110*, 23547–23556. (d) Wang, D.; Fu, Q.; Huang, J. *J. Appl. Polym. Sci.* **2006**, *101*, 509–514.
- (24) (a) Krafft, M. P.; Riess, J. G. *J. Polym. Sci., Part A: Polym. Chem.* **2007**, *45*, 1185–1198. (b) Shutt, E. G.; Klein, D. H.; Mattrey, R. M.; Riess, J. G. *Angew. Chem., Int. Ed.* **2003**, *42*, 3218–3235. (c) Riess, J. G. *Tetrahedron* **2002**, *58*, 4113–4131. (d) Riess, J. G. *Chem. Rev.* **2001**, *101*, 2797–2920. (e) Park, K.-H.; Berrier, C.; Lebaupain, F.; Pucci, B.; Popot, J.-L.; Ghazi, A.; F.; Zito, *Biochem. J.* **2007**, *403*, 183–187. (f) Ortial, S.; Durand, G.; Poeggeler, B.; Polidori, A.; Pappolla, M. A.; Böker, J.; Hardeland, R.; Pucci, B. *J. Med. Chem.* **2006**, *49*, 2812–2820. (g) Chaudier, Y.; Zito, F.; Barthélémy, P.; Stroebel, D.; Ameduri, B.; Popot, J.-L.; Pucci, B. *Bioorg. Med. Chem. Lett.* **2002**, *12*, 1587–1590.
- (25) Gentilini, C.; Boccalon, M.; Pasquato, L. *Eur. J. Org. Chem.* **2008**, 3308–3313.
- (26) Lucarini, M.; Franchi, P.; Pedulli, G. F.; Pengo, P.; Scrimin, P.; Pasquato, L. *J. Am. Chem. Soc.* **2004**, *126*, 9326–9329.

hexaethyleneglycol chains were also prepared, but their solubility in polar solvents is scarce.

Results and Discussion

MPC-F8-PEG Synthesis. Two main problems for the synthesis of MPC-F8-PEG nanoparticles were addressed in this work: (i) the low nucleophilicity of the sulfur atom of thiol **1** due to the withdrawing effect of the perfluorinated chain in α -position; (ii) the high hydrophobicity of the perfluorinated portion that strongly affects the solubility of Au NPs in polar solvents and eventually in aqueous media. As far as point (i) is concerned, the sulfur atom of thiol HS-F8-PEG presents a very low electronic density with respect to alkyl thiols. Indeed, preliminary experiments carried out to set up the experimental conditions for the synthesis of Au NPs in the presence of thiol **1** showed that the addition of the thiol to the tetrachloroaurate water solution is not accompanied by a change of color of the solution, from pale yellow to red-brown. This behavior suggests that the formation of the complex Au-SR with reduction of Au(III) to Au(I) does not occur. Subsequent addition of sodium boron hydride gives rise to insoluble aggregates.

To increase the nucleophilic character of the sulfur atom, we decided to use the thiolate in place of the thiol to promote the key step of reduction to Au(I), Scheme 1. This modification allowed us to obtain MPC-F8-PEG without formation of aggregates.

Another key point for the preparation of gold nanoparticles protected by amphiphilic fluorinated thiols was the solubility of the nanoparticles, which is limited both by the high hydrophobicity and by the lipophobicity of the fluorinated portion of the thiol. Thus, the poly(oxoethylene) chain of the thiol must be long enough to balance the effect of the eight CF_2 units. Fluorinated amphiphilic thiols **2–4** comprising short oligoethylene glycol portions were initially employed in the synthesis, giving rise to nanoparticles which were insoluble in water and only slightly soluble in organic solvents. This problem was successfully overcome by using HS-F8-PEG which contains a short PEG-OMe 550 chain. Indeed, MPC-F8-PEG is completely soluble in water, methanol, ethanol, trifluoroethanol, N,N' -dimethylformamide, dimethylsulfoxide, ethyl acetate, acetonitrile, acetone, dichloromethane, and chloroform. The Au nanoparticles are insoluble in diethylether and hydrocarbon solvents.

When we explored different reaction conditions for the synthesis of MPC-F8-PEG by using a molar ratio thiol **1**/Au = 0.7 and performing the reduction at room temperature, gold nanoparticles with an average core diameter of 2.9 nm were formed. Increasing the ratio thiol **1**/Au to 2.5:1 gives rise to nanoparticles with a core diameter of 1.6 nm, while a thiol **1**/Au molar ratio of 2:1 and reduction with NaBH_4 at 0 °C caused the nanoparticles to precipitate in the reaction medium. This may be likely due to the low solubility of the thiolate–Au(I) complex at low temperature. Indeed, by carrying out the reduction process at room temperature, this problem was overcome. We report here the complete characterization of nanoparticles obtained using a thiol **1**/Au molar ratio of 2:1 and by performing the reduction at room temperature.

MPC-F8-PEG Characterization. The average core diameter of the clusters determined by TEM analysis was 2.7 ± 0.6 nm (see Supporting Information, Figure S1). A TGA profile (Figure S2) shows weight loss at two different temperatures similarly

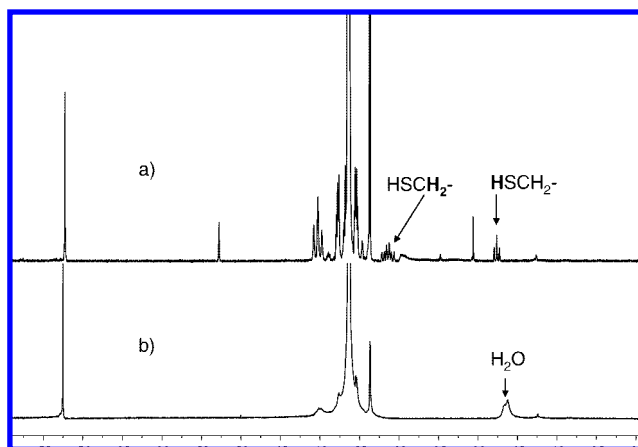


Figure 1. (a) ^1H NMR (CDCl_3 , 400 MHz) of HS-F8-PEG and (b) ^1H NMR (CDCl_3 , 400 MHz) of MPC-F8-PEG ($\delta = 1.6$ ppm: H_2O) prepared with a thiol **1**/Au ratio of 2:1.

to what already was observed with MPC-C8-TEG.²⁷ This suggests that the two step process is not peculiar for fluorinated MPCs but is associated with the presence of the poly(oxoethylene) chain. The organic content of the nanoparticles determined by TGA analysis was found to amount to 43%. Based on these data an average composition $\text{Au}_{670}(\text{S-F8-PEG})_{107}$ was calculated, which corresponds to a molecular weight of 231 600 Da. The relatively low number of thiolates per nanoparticle is in agreement with the fact that the van der Waals diameter of a perfluorocarbon chain is 5.7 Å whereas that of a hydrocarbon chain is 4.2 Å.²⁸ The absence of the SP band in the UV–vis spectrum (Figure S3) in methanol is consistent with the sharp size distribution of the core nanoparticles centered at 2.7 nm. The IR spectrum (Figure S4) shows the presence of the amphiphilic thiolate of **1** on the nanoparticles. The proton NMR spectrum of MPC-F8-PEG dissolved in deuterated chloroform (Figure 1b) shows the lack of the doublet of triplet at 3.11 ppm pertaining to the methylene next to sulfur, present in the spectrum of thiol **1** (Figure 1a), indicating the absence of free thiol.²⁹ This result is in agreement also with the ^{19}F NMR spectra (Figure S5) where the triplet of the CF_2 in α -position to the sulfur is absent in the spectrum of the MPC-F8-PEG.

MPC-F8-PEG were analyzed by XPS. To this purpose, as illustrated in Figure 2, we compared the binding energy of the Au 4f core level peaks of MPC-F8-PEG to those of gold nanoparticles protected by dodecanethiol (MPC-C12), for which synthesis and XPS characterization have been reported in the literature.¹ For the latter, XPS analysis reveals only one Au $4f_{7/2}$ core level component with a binding energy (BE) of 83.9 eV and hence supports the sole presence of Au(0) on the surface.³⁰

(27) Lucarini, M.; Franchi, P.; Pedulli, G. F.; Gentilini, C.; Polizzi, S.; Pengo, P.; Scrimin, P.; Pasquato, L. *J. Am. Chem. Soc.* **2005**, *127*, 16384–16385.

(28) Barriet, D.; Lee, T. R. *Curr. Opin. Colloid Interface Sci.* **2003**, *8*, 236–242.

(29) Terrill, R. H.; Postlethwaite, T. A.; Chen, C.; Poon, C.-D.; Terzis, A.; Chen, A.; Hutchison, J. E.; Clark, M. R.; Wignall, G.; Londono, J. D.; Superfine, R.; Falvo, M.; Johnson, C. S., Jr.; Samulski, E. T.; Murray, R. W. *J. Am. Chem. Soc.* **1995**, *117*, 12537–12548.

(30) Hostetler, M. J.; Wingate, J. E.; Zhong, C. J.; Harris, J. E.; Vachet, R. W.; Clark, M. R.; Londono, J. D.; Green, S. J.; Stokes, J. J.; Wignall, G. D.; Glish, G. L.; Porter, M. D.; Evans, N. D.; Murray, R. W. *Langmuir* **1998**, *14*, 17–30.

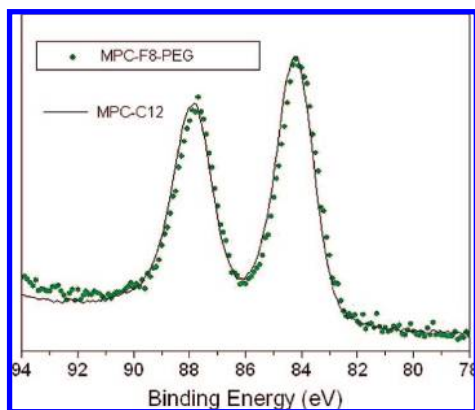


Figure 2. XPS Au 4f core level spectra of MPC-F8-PEG and MPC-C12.

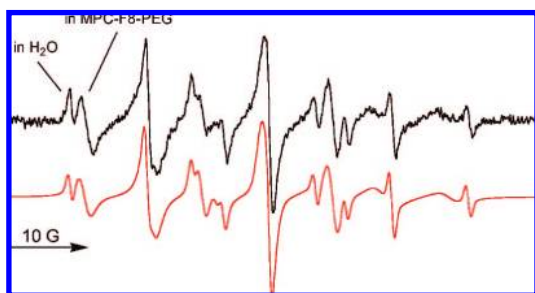


Figure 3. ESR spectrum of **6** recorded in the presence of MPC-F8-PEG 0.56 mM (in black) and the corresponding computer simulation (in red).

Table 1. ESR Parameters of **6** (1 G = 0.1 mT) and Partition Equilibrium (K_{eq}) Constants at 298 K

	$a(N)/G$	$a(2H_{\beta})/G$	g -factor	K_{eq}/M^{-1}
water ^a	16.25	10.14	2.0056	—
MPC-F8-TEG	15.46	8.68	2.0057	176
MPC-C8-TEG ^b	15.67	8.97	2.0057	87 ^c

^a Contains 10% (v/v) of methanol. ^b From ref 27. ^c See ref 33.

In fact, when gold is oxidized (Au(I)) a peak at ~ 1 eV higher BE (~ 85.1 eV) should be present.³¹

A Au 4f core level of MPC-F8-PEG and MPC-C12 appears as the typical metallic doublet with a $4f_{7/2}$ BE of 83.95 eV, as tabulated; no significant contribution seems to be present at the high BE tail. These data suggest that both MPC-F8-PEG and MPC-C12 have metallic Au atoms on the last shell.

We set up ESR spectroscopy experiments to investigate the properties of 3D-SAM a few years ago.^{26,27} The radical probe we used in this study is *para-n*-pentyl benzyl hydroxyalkyl nitroxide **6** (Chart 1). Figure 3 shows the ESR spectrum of nitroxide **6** generated directly inside an ESR tube by oxidizing the corresponding amines (1 mM) with Oxone (1 mM) in the presence of MPC-F8-PEG 0.56 mM at 298 K in water.

The spectrum is characterized by two sets of signals due to the radical partitioned in the monolayer in equilibrium with the free nitroxide. Inspection of Table 1 shows that both the values of $a(N)$ and of $a(2H_{\beta})$ decrease considerably when the aminoxyl is located in the less polar environment of the monolayer, giving rise to significant differences in the resonance fields for the $m_1(2H_{\beta}) = \pm 1$ lines of the two spectra. The reduction of

coupling constants, already reported in our previous studies of different MPC,^{26,27} has been attributed to the larger weight in media of low polarity of the nitroxide mesomeric forms in which the unpaired electron is localized on the oxygen rather on the nitrogen atom.³² Comparison of the values of both $a(N)$ and $a(2H_{\beta})$ for the radical located in the MPC-F8-PEG and MPC-C8-TEG monolayer indicates that they are substantially smaller in the former case (see Table 1). This difference is a consequence of the reduced polarity of the environment experienced by the nitroxide function when dissolved in the fluorinated amphiphilic monolayer.

The equilibrium constant, K_{eq} , for the partition of the probe between the water and the fluorinated monolayer was obtained by plotting the ratio between the concentration of the probe dissolved in the monolayer and that of the free species in water, obtained from the ESR spectra, against the concentration of S-F8-TEG (see Figure S6 in the Supporting Information). Comparison of the value found in the present work ($K_{eq} = 176 M^{-1}$) with that estimated for MPC-C8-TEG nanoparticles of the same size^{27,33} ($K_{eq} = 87 M^{-1}$) clearly indicates that the radical probe has a greater affinity for the fluorinated monolayer.

Exchange Reaction. A very important feature of gold nanoparticles is the possibility to introduce in the protecting monolayer other thiols (eventually containing the desired functional groups) by exchange of the thiolates present on the monolayer with different thiols.³⁴ We studied the exchange process using perfluorinated nanoparticles of different sizes and HS-C8-TEG as the entering thiol. For example, using a ratio of thiolates present on the monolayer and HS-C8-TEG of 1:1, after 72 h at 28 °C in methanol, nanoparticles with a mixed monolayer were obtained (MMPC-F8-PEG/C8-TEG). The composition of the monolayer has been determined by integration of the proton NMR spectrum of the nanoparticles (Figure S7). By exploring various reaction conditions the composition of the mixed monolayer may be tuned. These results will be reported elsewhere.³⁵

Conclusions

We have succeeded in synthesizing the first example of water-soluble gold nanoparticles protected by a monolayer of fluorinated amphiphilic thiols (MPC-F8-PEG). The solubility properties of the nanoparticles in connection with the intrinsic features of perfluorinated amphiphiles opens the way to possible applications in the medical field such as antioxidant carriers. Moreover, considering the ease of inserting other thiolates in the monolayer and the strong hydrophobicity of the perfluorinated region, these nanoparticles may become appealing examples of multicompartments nanoparticles with the capacity to

(31) Abis, L.; Armelao, L.; Belli Dell'Amico, D.; Calderazzo, F.; Garbassi, F.; Merigo, A.; Quadrelli, E. A. *J. Chem. Soc., Dalton Trans.* **2001**, 2704–2709.

(32) Lucarini, M.; Luppi, B.; Pedulli, G. F.; Roberts, B. P. *Chem.—Eur. J.* **1999**, 5, 2048–2054.

(33) We have previously shown that the solubilization of the organic probe in the monolayer strongly depends on the nanoparticle diameter. In particular, K_{eq} increases linearly as the nanoparticle diameter decreases. By making use of the equilibrium constants determined with MPC-C8-TEG nanoparticles of 1.6, 3.4, and 5.3 nm (ref 27), we estimated for MPC-C8-TEG nanoparticles having an average core diameter of 2.7 nm a value of $87 M^{-1}$.

(34) Hostetler, M. J.; Green, S. J.; Stokes, J. J.; Murray, R. W. *J. Am. Chem. Soc.* **1996**, 118, 4212–4213.

(35) Gentilini, C.; Franchi, P.; Mileo, E.; Polizzi, P.; Lucarini, M.; Pasquato L. Manuscript in preparation.

store and release active molecules. The potential of these new nanostructures is under active investigation in our laboratories.

Experimental Section

General. NMR spectra were recorded on a Jeol GX-400 MHz (operating at 400 MHz for ^1H) and on a Bruker Avance 300 MHz (operating at 282 MHz for ^{19}F) using CDCl_3 as a deuterated solvent. ^1H NMR spectra were referenced to the residual protons in the deuterated solvent. Data are reported as follows: chemical shifts are in ppm in the δ scale; multiplicity (s: singlet, d: doublet, t: triplet, q: quartet, br: broadband); integration; assignment. ^{19}F NMR spectra were referenced to trifluorotoluene as the external standard. FTIR spectra were recorded using a Thermo Nicolet Avatar 320 FT-IR spectrophotometer on NaCl disks. UV–visible spectra were collected on a UV–vis Unicam Helios β spectrophotometer. All reagents were purchased from Aldrich and used without further purification. Dry solvents were obtained from Fluka. Chlorinated solvents were stirred over K_2CO_3 for at least 24 h prior to use. All other solvents were reagent grade and used as received.

TGA Analysis. TGA analysis was performed on TGA Q-500 V6.3 Build 189 using a heating rate of $10\text{ }^\circ\text{C}/\text{min}$ up to $1000\text{ }^\circ\text{C}$.

TEM Analysis. TEM images were obtained with a Jeol 3010 high resolution electron microscope (1.7 nm point-to-point) operating at 300 keV using a Gatan slow-scan CCD camera (mod. 794). TEM samples of protected gold nanoparticles were prepared by placing a single drop of 0.5 mg/mL isopropanol dispersion onto a 200-mesh copper grid coated with an amorphous carbon film. The grid was then dried in air for 24 h. Depending on the Au core size, magnifications between 250000 and 600000 were used for counting purposes. Diameters were measured manually using Gatan software Digital Micrograph (ver. 3.4.1) on at least 300 particles.

XPS Measurements. Ag foil (purity 99.99%, Goodfellow, U.K.) was used as a substrate. It was polished (Brasso metal polish, Reckitt Benckiser UK Ltd., U.K.) to remove most of the impurities from the surface, sonicated in ethanol for 20 min, and dried in an oven (Thermo Electron Corporation, U.S.A.) at $65\text{ }^\circ\text{C}$ immediately before being employed. The samples were dissolved in dichloromethane (purity 99.99%, ACROS, Belgium), then a drop was cast on the substrate and left to dry. All samples contain oxygen from exposure to ambient air and also from the residual contamination of the substrate. Each sample was introduced through a load lock system into an SSX-100 (Surface Science Instruments) photoelectron spectrometer with a monochromatic Al $\text{K}\alpha$ X-ray source ($h\nu = 1486.6\text{ eV}$). The base pressure in the spectrometer was 6×10^{-10} mbar during the measurements. The energy resolution was set to 1.7 eV to minimize data acquisition time, and the photoelectron takeoff angle was 37° . The binding energies were referenced to the Ag 3d core level of the substrate (tabulated value: Ag 3d $_{5/2} = 368.27\text{ eV}$).³⁶

EPR Measurements. Radical (*para-n*-pentyl-benzyl)-1-hydroxy-2-methyl-2-propylnitroxide (**6**) was generated by mixing 0.5 μL of a methanol solution containing the corresponding amine (0.1 M) and 0.5 μL of a water solution containing Oxone (0.1 M) with 100 μL of a water solution containing variable amounts of MPC-F8-PEG. Samples were transferred in capillary tubes (diameter 1 mm) and then placed inside the thermostatted cavity of the EPR spectrometer. EPR spectra were collected using a Bruker ESP300 spectrometer equipped with an NMR gaussmeter for field calibration and a Hewlett-Packard 5350B microwave frequency counter for the determination of the g -factors, which were referenced to that of the perylene radical cation in concentrated H_2SO_4 ($g = 2.00258$). The sample temperature was controlled with a standard variable

temperature accessory and monitored before and after each run using a copper-constantan thermocouple. The instrument settings were as follows: microwave power 5.0 mW, modulation amplitude 0.05 mT, modulation frequency 100 kHz, scan time 180 s. Digitized EPR spectra were transferred to a personal computer for analysis using digital simulations carried out with a program developed in our laboratory and based on a Monte Carlo procedure.³² The input data for the program are the number of nonequivalent nuclei, the hyperfine splitting constants of the free and included radical, the intrinsic line width in the absence of exchange, and the rate constants for the exchange process.

Preparation of Thiolate Solution. Thiol **1** (243 mg, 0.233 mmol), prepared as previously described,²⁵ was dissolved in 3 mL of dry, deoxygenated methanol, under an argon atmosphere. To the mixture, 0.8 mL of 0.5 M sodium methoxide in methanol was added. The solution was stirred for 30 min before use.

Synthesis of MPC-F8-PEG. We slightly modified the procedure reported previously for the synthesis of 2 nm water soluble gold nanoparticles.¹⁰ $\text{HAuCl}_4 \cdot 3\text{H}_2\text{O}$ (46 mg, 0.117 mmol) was dissolved in 23 mL of bidistilled water and poured into a 100 mL round-bottom flask. The solution of thiolate **1** (2 equiv) was added to the mixture through a double-tipped needle under an argon atmosphere. The solution was stirred at room temperature for 1 h. Then, NaBH_4 (50 mg, 1.33 mmol) dissolved in 3.3 mL of bidistilled water was added in 10 s. The solution color turned deep-brown, suggesting formation of small protected nanoparticles. The mixture was left stirring for 3 h, and then the solvent was removed under reduced pressure. The residue was transferred into a centrifuge tube, dispersed in Et_2O , and repeatedly washed ($7 \times 20\text{ mL}$) by centrifugation at 4000 rpm to remove unbound thiol. The precipitate was recovered as a brown solid (41 mg). IR (CDCl_3) ν (cm^{-1}): 3400, 2874, 2245, 1461, 1350, 1211, 1145. ^1H NMR (CDCl_3 , 400 MHz) δ : 3.3 (br, CH_3O); 3.5–3.6 (br, CH_2O); 4.0 (br, $\text{CF}_2\text{CH}_2\text{O}$). ^{19}F NMR (CDCl_3 , 300 MHz) δ : -123.9 (br, CF_2); -123.2 (br, CF_2); -122.3 (br, CF_2); -120.3 (br, $\text{CF}_2\text{CH}_2\text{O}$). UV–vis (MeOH, $c = 0.1\text{ mg/mL}$): monotonic decay from 200 nm. TGA: 43%.

Synthesis of MMPC-C8-TEG/F8-PEG = 1/1 by Place-Exchange Reaction. MPC-F8-PEG ($d = 1.6\text{ nm}$), 17 mg, was dissolved in 19 mL of deoxygenated methanol, under an argon atmosphere. A solution of 3 mg (9.4 mmol) of HS-C8-TEG in 1 mL of methanol was added, and the mixture was kept at $28\text{ }^\circ\text{C}$ for 3 days. The solvent was removed under reduced pressure, and the Au NPs were repeatedly washed with diethyl ether and centrifuged at 4000 rpm. The Au NPs were dissolved in methanol and permeated on Sephadex LH-20 using methanol as eluent. 15 mg of nanoparticles were obtained as a brown solid.

^1H NMR (CDCl_3 , 400 MHz) δ : 1.1–1.6 (CH_2); 2.2 (CH_2CO); 3.3 (CH_3O); 3.5–3.6 (CH_2O); 4.0 ($\text{CF}_2\text{CH}_2\text{O}$). TEM: $d_m = 1.6\text{ nm}$; $\sigma = 0.2\text{ nm}$; $n = 300$. TGA: 62%.

Acknowledgment. We thank Dr. Fabrizio Mancin for ^{19}F NMR spectra and Prof. Stefano Polizzi for TEM analysis. Financial support from MUR, PRIN 2006 (Prot. 2006039071), and Progetto Regione FVG 2005. Additional support came from the Dutch Foundation for Fundamental Research on Matter (FOM) and from the Breedtestrategie program of the University of Groningen.

Supporting Information Available: TEM and TGA analyses, UV–vis, IR, and ^{19}F NMR spectra of MPC-F8-PEG; plot for determination of K_{eq} for the probe **6** from ESR spectra and ^1H NMR spectrum of MMPC-F8-PEG/C8-TEG. This material is available free of charge via the Internet at <http://pubs.acs.org>.

(36) Seah, M. P. *Surf. Interface Anal.* **1989**, *14*, 488.